

Contribution from the Department of Chemistry, University of Missouri—Rolla, Rolla, Missouri 65401, and the Istituto di Fisica, the Istituto di Chimica Generale e Inorganica, the Centro di Ricerche sui Biopolimeri del CNR, and the Istituto di Chimica e Tecnologia dei Radioelementi del CNR, I-35100 Padua, Italy

A Mössbauer, Magnetic, and Single-Crystal X-ray Structural Study of *trans*-Bis(4-acetylpyridine)diaquobis(isothiocyanato)iron(II)

GARY J. LONG,* GIUSEPPE GALEAZZI, UMBERTO RUSSO, GIOVANNI VALLE, and SANDRO CALOGERO

Received April 12, 1982

The single-crystal X-ray structure of *trans*-bis(4-acetylpyridine)diaquobis(isothiocyanato)iron(II) reveals an all-*trans* pseudooctahedral coordination geometry. The acetyl oxygen atoms are not coordinated but are hydrogen bonded to the water molecules in an adjacent molecule. The thiocyanate anion is coordinated through the nitrogen atom in an essentially linear fashion. An intermolecular hydrogen bond connects the coordinated water oxygen to the 4-acetylpyridine oxygen. The iron(II) to coordinated nitrogen and oxygen bond distances are typical of high-spin iron(II) and are consistent with magnetic studies, which reveal paramagnetic behavior down to 4.2 K. The high-spin electronic configuration is also confirmed by the optical spectrum and by Mössbauer spectral studies, which indicate a negative quadrupole interaction and a typical high-spin(II) isomer shift. This is the first reported complex with three different ligands coordinated to a high-spin iron(II) ion.

Introduction

Iron(II) complexes with various pyridine-related ligands have been studied by infrared,¹⁻³ optical,⁴ and Mössbauer-effect spectroscopy⁵⁻¹⁵ and by magnetic susceptibility,^{16,17} thermal,¹⁰ and single-crystal X-ray techniques.^{18,19} In general, these complexes are either bis or tetrakis complexes.

The bis complexes, of stoichiometry FeL_2X_2 , where L is a pyridine-related ligand and X is a halide or pseudohalide, may have either a tetrahedral or polymeric linear-chain octahedral coordination geometry with bridging anions.²⁰ The tetrakis complexes generally adopt the tetragonally distorted *trans* octahedral geometry.¹⁹ In particular, X-ray studies¹⁸ on $\text{Fe}(\text{py})_4(\text{NCS})_2$ and related complexes have indicated a nitrogen-coordinated thiocyanate ligand.

In an attempt to further study the coordinating ability of related substituted pyridines and the bonding mode of the thiocyanate ligand, we have obtained and characterized a new complex, $\text{Fe}(\text{4-acetylpyridine})_2(\text{H}_2\text{O})_2(\text{NCS})_2$, which we abbreviate as $\text{Fe}(\text{4-acpy})_2(\text{H}_2\text{O})_2(\text{NCS})_2$. Each of the ligands assumes the *trans* position, and to our knowledge, this is the first complex with three different ligands coordinated to an iron(II) ion.

Experimental Section

The complex $\text{Fe}(\text{4-acpy})_2(\text{H}_2\text{O})_2(\text{NCS})_2$, which crystallized as deep red well-shaped crystals, was obtained during an attempt to prepare $\text{Fe}(\text{4-acpy})_2(\text{NCS})_2$ by the reported methods.⁸ A comparison among infrared, Mössbauer, and magnetic data reveals that the two compounds are indeed different. The elemental analysis and the water content, as determined by the Karl Fischer method, indicate the presence of two water molecules and the formula $\text{Fe}(\text{4-acpy})_2(\text{H}_2\text{O})_2(\text{NCS})_2$. Anal. Calcd for $\text{FeC}_{16}\text{H}_{18}\text{N}_4\text{O}_4\text{S}_2$: Fe, 12.4; C, 42.7; H, 4.0; N, 12.4; H_2O , 7.1. Found: Fe, 12.5; C, 42.3; H, 3.9; N, 12.3; H_2O , 7.2. The presence of water in the complex is shown in the infrared spectrum by the strong absorption at 3336 cm^{-1} . Many attempts to remove the water molecules in order to obtain $\text{Fe}(\text{4-acpy})_2(\text{NCS})_2$ were unsuccessful. Decomposition was observed at 100°C under vacuum. Only a partial dehydration was observed at room temperature with P_2O_5 under vacuum.

Physical Measurements. The magnetic measurements were made on a Faraday balance, which utilizes a Janis Supravertemp helium cryostat and a Lake Shore Cryotronics temperature controller.²¹ The balance was calibrated with $\text{CuSO}_4 \cdot 5\text{H}_2\text{O}$ and $\text{CoHg}(\text{NCS})_4$. The conductivity was measured on an LKB 3216B bridge at 25°C in a conventional closed cell by using a $10^{-3}\text{ mol dm}^{-3}$ solution in MeNO_2 . The infrared spectra were obtained on a Perkin-Elmer 580 spectrophotometer by using KBr pellets or Nujol mulls. The electronic

absorption spectrum was recorded on a Beckman DK 2A spectrometer as a Nujol mull.

The Mössbauer spectra were obtained on a Harwell constant-acceleration spectrometer, which utilized a room-temperature rhodium matrix source and was calibrated with natural α -iron foil. The helium-temperature spectra were obtained in a cryostat in which the sample was placed directly in the liquid helium. The magnetically perturbed spectra were obtained with a superconducting magnet, which produced a transverse magnetic field. The Mössbauer spectra were evaluated by using least-squares minimization computer programs. The differential thermal gravimetric results were obtained on a Mettler differential thermal analyzer.

Crystallographic Data and Refinement of the Structure. The crystal structure of $\text{Fe}(\text{4-acpy})_2(\text{H}_2\text{O})_2(\text{NCS})_2$ is monoclinic in the space group $P2_1/a$ with $a = 10.405(2)\text{ \AA}$, $b = 16.304(1)\text{ \AA}$, $c = 6.360(3)\text{ \AA}$, $\beta = 107.3(1)^\circ$, $V = 1030.1\text{ \AA}^3$, and $Z = 2$. The calculated density is 1.45 g/cm^3 , and the measured density is 1.46 g/cm^3 .

Intensity data were collected on a four-circle Philips PW 1100 diffractometer with graphite-monochromated $\text{Mo K}\alpha$ radiation ($\lambda = 0.7107\text{ \AA}$, $\mu = 2.79\text{ cm}^{-1}$) in the range $2 < 2\theta < 26^\circ$, by using the $\theta/2\theta$ scan mode. The intensities of 2018 independent reflections were measured, and 1440 with intensity above $3\sigma(I)$ were used in subsequent calculations. The data were corrected for Lorentz and polarization effects.

The structure was solved by the heavy-atom method, with the iron

- Frank, C. W.; Rogers, L. B. *Inorg. Chem.* **1966**, *5*, 615.
- Gill, N. C.; Nuttal, R. H.; Scaife, D. E.; Sharp, D. W. A. *J. Inorg. Nucl. Chem.* **1961**, *18*, 79.
- Goldstein, M.; Unsworth, W. D. *Spectrochim. Acta, Part A* **1972**, *28A*, 1297.
- Goodgame, D. M. L.; Goodgame, M.; Hitchman, M. A.; Weeks, M. J. *Inorg. Chem.* **1966**, *5*, 635.
- Tominaga, T.; Takeda, M.; Morimoto, T.; Saito, N. *Bull. Chem. Soc. Jpn.* **1970**, *43*, 1093.
- Golding, R. M.; Mok, K. F.; Duncan, J. F. *Inorg. Chem.* **1966**, *5*, 774.
- Little, B. F.; Long, G. J. *Inorg. Chem.* **1978**, *17*, 3401.
- Wei, H. H.; Ho, Y. S. *Inorg. Chim. Acta* **1979**, *34L*, 185.
- Wei, H. H.; Men, L. C. *J. Inorg. Nucl. Chem.* **1978**, *40*, 221.
- Takeda, M.; Tominaga, T.; Saito, N. *J. Inorg. Nucl. Chem.* **1974**, *36*, 2459.
- Reiff, W. M.; Frankel, R. B.; Little, B. F.; Long, G. J. *Inorg. Chem.* **1974**, *13*, 2153.
- Merrithew, P. B.; Rasmussen, P. G.; Vincent, D. H. *Inorg. Chem.* **1971**, *10*, 1401.
- Sanchez, J. P.; Asch, L.; Friedt, J. M. *Chem. Phys. Lett.* **1974**, *28*, 68.
- Reiff, W. M.; Frankel, R. B.; Little, B. F.; Long, G. J. *Chem. Phys. Lett.* **1974**, *28*, 68.
- Burbridge, C. D.; Goodgame, D. M. L. *Inorg. Chim. Acta* **1970**, *4*, 231.
- Long, G. J.; Baker, W. A., Jr. *J. Chem. Soc. A* **1971**, 2956.
- Gerloch, J. M.; McMeeking, R. F.; White, A. M. *J. Chem. Soc., Dalton Trans.* **1975**, 2452.
- Søtofte, I.; Rasmussen, S. E. *Acta Chem. Scand.* **1967**, *21*, 2028.
- Long, G. J.; Clarke, P. J. *Inorg. Chem.* **1978**, *17*, 1394.
- Porai-Koshits, M. A.; Tishchenko, G. N. *Sov. Phys.—Crystallogr. (Engl. Transl.)* **1960**, *4*, 216.
- Long, G. J.; Longworth, G.; Battle, P.; Cheetham, A. K.; Thundathil, R. V.; Beveridge, D. *Inorg. Chem.* **1979**, *18*, 624.

* To whom all correspondence should be addressed at the University of Missouri—Rolla.

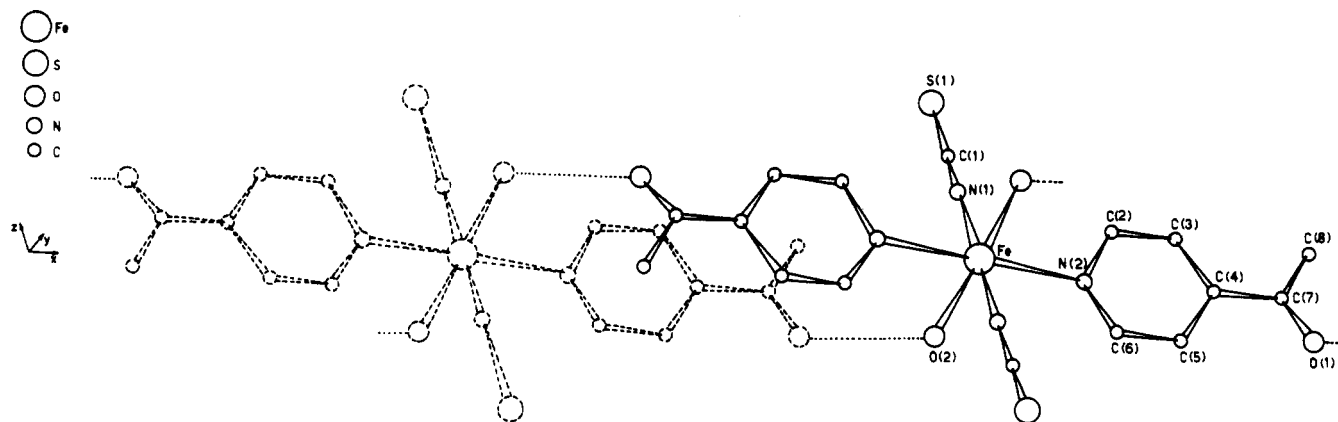


Figure 1. Perspective view of $\text{Fe}(4\text{-acpy})_2(\text{H}_2\text{O})_2(\text{NCS})_2$ and its crystallographically related hydrogen-bonded neighbor.

Table I. Atomic Coordinates and Thermal Parameters ($\times 10^4$)

atom	<i>x/a</i>	<i>y/b</i>	<i>z/c</i>	<i>U</i> (11)	<i>U</i> (22)	<i>U</i> (33)	<i>U</i> (23)	<i>U</i> (13)	<i>U</i> (12)
Fe	0000	0000	0000	467 (4)	486 (4)	416 (4)	-68 (4)	168 (3)	-28 (4)
S(1)	39 (2)	2191 (1)	5193 (2)	1869 (15)	486 (6)	591 (7)	-121 (6)	485 (8)	105 (9)
O(1)	6081 (3)	858 (2)	-2618 (5)	530 (15)	669 (19)	774 (19)	37 (16)	297 (14)	-1 (14)
O(2)	-1273 (3)	715 (2)	-2675 (5)	500 (17)	671 (20)	538 (16)	59 (14)	182 (13)	22 (15)
N(1)	27 (3)	969 (2)	2194 (5)	617 (20)	586 (21)	593 (20)	-165 (17)	269 (16)	-60 (17)
N(2)	1860 (3)	509 (2)	-591 (5)	441 (16)	467 (17)	424 (16)	2 (13)	110 (13)	-14 (13)
C(1)	32 (4)	1473 (2)	3426 (3)	609 (23)	499 (23)	488 (21)	000 (18)	228 (18)	-59 (18)
C(2)	2710 (4)	964 (2)	928 (6)	512 (21)	544 (24)	527 (22)	-101 (19)	194 (18)	-29 (18)
C(3)	3941 (4)	1223 (2)	786 (7)	501 (21)	501 (24)	578 (24)	-139 (20)	113 (19)	-52 (19)
C(4)	4344 (3)	983 (2)	-1004 (6)	425 (18)	355 (19)	553 (21)	85 (16)	113 (16)	42 (15)
C(5)	3457 (4)	516 (2)	-2609 (6)	514 (21)	570 (24)	415 (20)	40 (18)	163 (17)	-22 (18)
C(6)	2239 (4)	301 (2)	-2359 (6)	505 (21)	580 (22)	387 (19)	-22 (17)	132 (16)	-53 (18)
C(7)	5698 (4)	1191 (2)	-1216 (7)	436 (19)	452 (22)	620 (24)	125 (19)	112 (18)	18 (17)
C(8)	6546 (5)	1815 (4)	315 (10)	530 (27)	730 (35)	854 (37)	-1 (30)	157 (25)	-147 (26)

atom	<i>x/a</i>	<i>y/b</i>	<i>z/c</i>	<i>U</i> , Å ²	atom	<i>x/a</i>	<i>y/b</i>	<i>z/c</i>	<i>U</i> , Å ²
H(2)	2427 (33)	1111 (21)	2177 (56)	476 (102)	H(82)	7335 (51)	1922 (29)	-121 (78)	953 (161)
H(3)	4456 (36)	1493 (23)	1894 (59)	530 (111)	H(83)	6138 (52)	2288 (33)	132 (84)	1021 (207)
H(5)	3705 (39)	358 (24)	-3831 (65)	686 (125)	H(O1)	-2084 (49)	822 (28)	-2759 (72)	845 (161)
H(6)	1633 (38)	-55 (23)	-3465 (61)	632 (111)	H(O2)	-984 (53)	1146 (32)	-3048 (83)	1012 (201)
H(81)	6776 (48)	1623 (30)	1807 (82)	965 (178)					

on the inversion center. Subsequent Fourier maps revealed all non-hydrogen atoms, and the anisotropic full-matrix least-squares refinement on *F* was carried out. The function $\sum [|F_o| - |F_c|]^2$, in which $w = 1$, was minimized, and the usual scattering factors were used.²² The hydrogen atoms were found on difference Fourier maps and were isotropically refined on the last full cycle. The final conventional *R* factor was 0.039. A perspective view of the molecular geometry together with its atomic numbering is shown in Figure 1. The final atomic coordinates and the thermal parameters are listed in Table I. Tables of observed and calculated structure factors are available as supplementary materials. Bond distances and angles are reported in Table II. The SHELX-76 system of programs²³ was used on a CDC Cyber 76 computer in the refinement of the structure.

Results and Discussion

The complex $\text{Fe}(4\text{-acpy})_2(\text{H}_2\text{O})_2(\text{NCS})_2$ consists of discrete molecules in which the iron-iron distance is greater than 5.2 Å and the iron coordination geometry is trans octahedral. The nonionic nature of the complex agrees with its conductivity value of $81.6 \Omega^{-1} \text{cm}^2 \text{mol}^{-1}$ obtained in MeNO_2 . The infrared data also indicate a N-bonded thiocyanate because of the presence of three characteristic bands: a strong sharp ν_{NCS} band at 2089cm^{-1} , with a shoulder at 2045cm^{-1} , a weak ν_{NCS} band at 798cm^{-1} , and a strong δ_{NCS} band at 471cm^{-1} .

Iron, which occupies the special position $\bar{1}$ in the crystal, has bond angles that range from 88.5° to 91.5° and bond

Table II. Bond Distances and Angles

Bond Distances, Å			
Fe-O(2)	2.160 (3)	C(3)-C(4)	1.381 (5)
Fe-N(1)	2.102 (3)	C(4)-C(7)	1.494 (5)
Fe-N(2)	2.237 (3)	C(7)-O(1)	1.208 (4)
N(1)-C(1)	1.135 (4)	C(7)-C(8)	1.501 (6)
C(1)-S(1)	1.622 (4)	C(4)-C(5)	1.383 (5)
N(2)-C(2)	1.326 (4)	C(5)-C(6)	1.369 (5)
C(2)-C(3)	1.376 (5)	C(6)-N(2)	1.342 (4)

Bond Angles, deg			
O(2)-Fe-N(1)	90.1 (1)	C(4)-C(7)-O(1)	119.5 (4)
N(2)-Fe-O(2)	91.5 (1)	O(1)-C(7)-C(8)	121.6 (4)
N(1)-Fe-N(2)	89.5 (1)	C(8)-C(7)-C(4)	118.9 (4)
Fe-N(1)-C(1)	177.7 (3)	C(7)-C(4)-C(5)	119.9 (3)
N(1)-C(1)-S(1)	179.8 (1)	C(3)-C(4)-C(5)	117.7 (3)
Fe-N(2)-C(2)	120.6 (2)	C(4)-C(5)-C(6)	119.5 (4)
N(2)-C(2)-C(3)	123.8 (4)	C(5)-C(6)-N(2)	123.1 (4)
C(2)-C(3)-C(4)	118.9 (4)	C(6)-N(2)-C(2)	116.9 (3)
C(3)-C(4)-C(7)	122.4 (3)	C(6)-N(2)-Fe	122.2 (2)

distances from 2.102 to 2.237 Å. Details of the bond distances and angles are given in Table II. The Fe-N(4-acpy) and Fe-N(thiocyanate) bond distances are reasonable for iron(II) in the high-spin electronic configuration and agree well with earlier results for pyridine complexes.^{18,19} The Fe-O(water) bond distance is somewhat longer than usual as a result of the presence of hydrogen bonding. Each $\text{Fe}(4\text{-acpy})_2(\text{H}_2\text{O})_2(\text{NCS})_2$ molecule is linked to two other crystallographically identical molecules by a 2.77-Å hydrogen bond, which connects the coordinated acetyl oxygen atoms in acetylpyridine in the two adjacent molecules.

(22) "International Tables for X-ray Crystallography"; Kynoch Press: Birmingham, U.K., 1962; Vol. 3.

(23) Sheldrick G. "SHELX 76 System of Computing Programs", Cambridge University, 1976.

Table III. Differential Thermal Gravimetric Analytical Results^a

t(DTA), °C			wt loss, mg	% wt loss		comments
initial	max	end		obsd	calcd	
80	100	115 (en)	2.95	8.04	8.00	loss of two H ₂ O's
203	215	225 (en)	4.20	11.4	9.87	loss of 1st acpy
410	430	450 (en)	~7.0	19.1		loss of 2nd acpy; dec of Fe(NCS) ₂
550	560	575 (en)	~2.0	5.4		continuous wt loss above 410 °C

^a Obtained in helium on 36.7 mg.

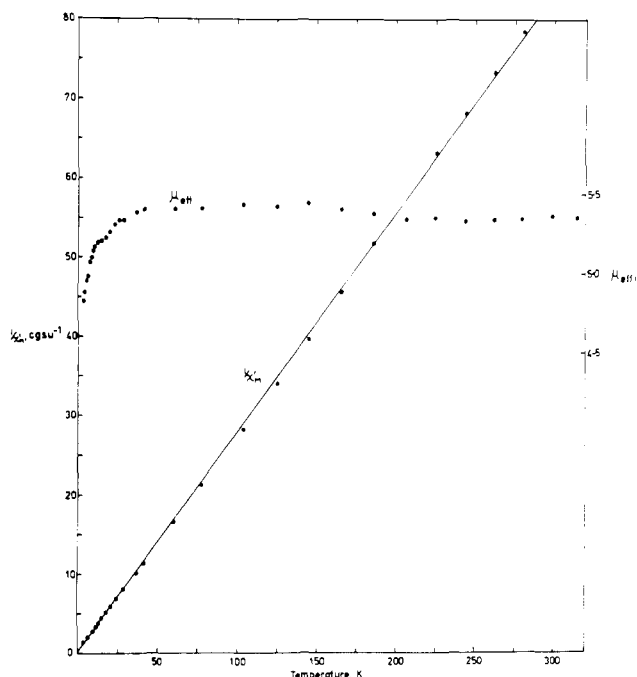


Figure 2. Inverse molar magnetic susceptibility and magnetic moment for Fe(4-acpy)₂(H₂O)₂(NCS)₂ as a function of temperature.

The 4-acpy ligand exhibits a typical ν_{C-O} vibrational band at 1682 cm⁻¹ which is shifted from its position at 1696 cm⁻¹ in the neat ligand.²⁴ This 14-cm⁻¹ shift confirms both the uncoordinated nature of the acetyl oxygen and its participation in a strong hydrogen bond. Typically the ν_{C-O} band shifts 3–10 cm⁻¹ if the carbonyl is hydrogen bonded.²⁴ The somewhat larger shift in this case reveals the strength of the hydrogen bonding as confirmed by the short oxygen–oxygen distance (see above). The dihedral angle between the 4-acpy plane and the FeN₄ plane is 22.48°, a value much smaller than the 51.11° found in Fe(py)₄Cl₂.¹⁹ This small value indicates the importance of the two coordinated water molecules in determining the orientation of the 4-acpy ring.

Differential Thermal Gravimetric Results. A differential thermal gravimetric analysis was carried out in helium in order to determine how well the water molecules were bound to the iron(II) center. The results of this analysis are presented in Table III and indicate a strong endotherm centered at 100 °C associated with the loss of the water molecules. A second sharp endotherm centered at 215 °C is associated with the loss of the first 4-acpy ligand. Above 225 °C the molecule slowly decomposes. These results indicate that water is rather strongly bonded to the complex.

Magnetic Measurements. The inverse magnetic susceptibility and the magnetic moment for Fe(4-acpy)₂(H₂O)₂(NCS)₂ are shown in Figure 2, and numerical values are given in Table

Table V. Mössbauer-Effect Spectral Results for Fe(4-acpy)₂(H₂O)₂(NCS)₂^a

T, K	δ	ΔE_Q	Γ	area ^b	χ^2
4.2	1.26	1.88	0.32	7.5	1.18
20	1.26	1.85	0.31	7.2	1.18
78	1.26	1.94	0.29	6.0	1.18
100	1.21	1.93	0.29	4.6	1.16
160	1.22	1.81	0.29	4.2	1.15
250	1.21	1.78	0.24	4.2	1.20
295	1.16	1.72	0.24	2.7	1.20

^a All data in mm/s relative to natural α -iron foil. ^b Total area in % mm/s.

IV (available as supplementary material). As is apparent from Figure 2, the magnetic susceptibility shows Curie law behavior from room temperature to 4.2 K, with a Curie-Weiss temperature of -0.45 K. The magnetic moment remains approximately constant at 5.3–5.4 μ_B down to ca. 20 K and then decreases slowly to 4.83 μ_B at 4.2 K. Although this decrease may be the result of a significant zero-field splitting, it seems more likely that it arises from a low-symmetry component in the ligand field potential. Calculations made by using the model of Figgis et al.²⁵ reveal a good agreement with the experimental results for an orbital reduction factor of 0.92, a spin-orbit coupling constant of ca. -70 cm⁻¹, and a distortion parameter of ca. 950 cm⁻¹. These values are typical of distorted high-spin iron(II) complexes¹⁶ but the specific values probably mean little because of the high correlation between the parameters and the low-symmetry of the complex. They do, however, illustrate that the decrease in μ_{eff} below ca. 20 K need not arise from any intermolecular magnetic coupling. Such magnetic coupling would not be expected in this case because the only exchange pathway would be via the hydrogen bonding between water and the acetyl oxygen on the ligand. The contribution of this pathway to any magnetic coupling would be expected to be very small.

Electronic Spectra. The electronic spectrum of Fe(4-acpy)₂(H₂O)₂(NCS)₂ exhibits a strong charge-transfer band beginning at ca. 16 000 cm⁻¹. In addition, a much weaker ligand field band is observed at 11 800 cm⁻¹ and a distinct shoulder is found at ca. 9500 cm⁻¹. The areas of the two bands are essentially equivalent. Although the specific assignments of these lines to the ⁵A₁ or ⁵B₁ states (derived from the ⁵E_g state in octahedral symmetry) is not certain, we can say that the average ligand field potential in Fe(4-acpy)₂(H₂O)₂(NCS)₂ is very similar to that in Fe(py)₄(NCS)₂ and Fe(py)₄(NCSe)₂.⁷ This indicates that the contribution of water to the ligand field potential is similar to that of pyridine. Unfortunately, because the complex contains three different ligands, it is difficult to draw any conclusion about their relative σ -bonding ability.

Mössbauer Spectral Results. The Mössbauer-effect spectral data for Fe(4-acpy)₂(H₂O)₂(NCS)₂ are presented in Table V. In these fits, it was assumed that the two components of the quadrupole doublet have the same area and line width. No significant improvement in χ^2 was observed if this constraint was removed. The spectral parameters are accurate to ca. ± 0.02 mm/s. A plot of the spectra obtained at several temperatures and in a 6-T applied magnetic field is presented in Figure 3. As has been observed in other tetrakis(pyridine) complexes,⁷ no magnetic ordering was observed in Fe(4-acpy)₂(H₂O)₂(NCS)₂ down to 1.6 K. Indeed, even the application of a 6-T applied magnetic field at 1.6 K does not induce any long-range magnetic order; the observed internal hyperfine field is essentially the applied magnetic field. If magnetic ordering were present, a Mössbauer transition from a quadrupole doublet paramagnetic spectrum to a six-line

(24) Bellamy, L. J. "The Infrared Spectra of Complex Molecules", 2nd ed.; Chapman and Hall: New York, 1980; Vol. 2, p 157.

(25) Figgis, B. N.; Lewis, J.; Mabbs, F. E.; Webb, G. A. *J. Chem. Soc.* A 1967, 442.

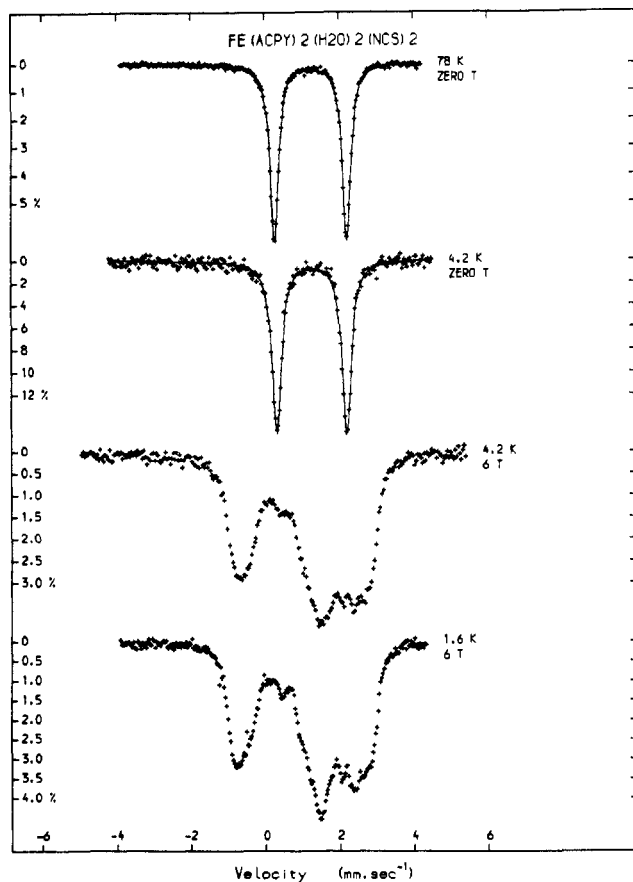


Figure 3. Mössbauer-effect spectra of $\text{Fe}(\text{4-acpy})_2(\text{H}_2\text{O})_2(\text{NCS})_2$ obtained at several temperatures and in a 6-T transverse applied magnetic field.

magnetic spectrum, at a well-defined Curie or Néel temperature, would be expected.

In order to determine the sign of the electric field gradient tensor, we have measured the spectrum of $\text{Fe}(\text{4-acpy})_2(\text{H}_2\text{O})_2(\text{NCS})_2$ in transverse and longitudinal magnetic fields

of 2.5, 3, 5, and 6 T at 4.2 K. Although the resolution of the individual components is poor, it is clear at all applied fields that the high-velocity line splits into a triplet while the low-velocity line splits into a doublet. This implies that the quadrupole coupling constant and hence the principal component of the electric field gradient tensor are negative and that the molecule has a small, nonzero asymmetry parameter, η . As is usual for high-spin iron(II) compounds with a large valence contribution to the electric field gradient, the quadrupole splitting increases with decreasing temperature down to 78 K. Below this temperature the quadrupole splitting unexpectedly decreases again. This decrease may be an indication of a low-temperature structural phase change between 78 and 20 K. A further indication of this phase change is seen in the magnetic moment (see Figure 2), which shows a small drop at ca. 25 K. In $\text{Fe}(\text{4-acpy})_2(\text{H}_2\text{O})_2(\text{NCS})_2$ the local site symmetry is only D_{2h} , so it is difficult to assign the orientation of the principal axis of the electric field gradient tensor, V_{zz} , with respect to the molecular geometry. It is possible to rationalize the observed negative quadrupole interaction in terms of a distortion with axial elongation along the "pseudotetragonal" $\text{N}(\text{acpy})\text{-Fe-N}(\text{acpy})$ axis, which is approximately parallel to the crystallographic a axis. Hence, V_{zz} would lie in a cone oriented along this axis. This pseudoaxial field partially lifts the degeneracy of the lowest $|xz\rangle$ and $|yz\rangle$ doublet and places the $|xy\rangle$ singlet several hundred wavenumbers higher in energy. This would produce the observed negative quadrupole interaction of the proper magnitude.

Acknowledgment. We wish to thank Mr. L. Badan, G. Bressanini, B. Laundry, L. Becker, S. M. Tetrick, and H. Rice for technical assistance. This investigation was supported by the National Science Foundation (Grant INT-8202403) and the Italian National Research Council under the U.S.-Italy Cooperative Science Program. U.R. thanks the ICTR-CNR of Padua for support.

Registry No. $\text{Fe}(\text{4-acpy})_2(\text{H}_2\text{O})_2(\text{NCS})_2$, 83510-92-3.

Supplementary Material Available: Table IV, giving magnetic susceptibility data, and a listing of structure factor amplitudes (10 pages). Ordering information is given on any current masthead page.